Title:

Naked mole-rat transcriptome signatures of socially-suppressed sexual maturation and links of reproduction to aging

Authors:

Martin Bens[a,1], Karol Szafranski[a,1], Susanne Holtze[b], Arne Sahm[a], Marco Groth[a], Hans A. Kestler[a,c], Thomas B. Hildebrandt[b,2], Matthias Platzer[a,2]

Affiliations:

[a] Leibniz Institute on Aging - Fritz Lipmann Institute, Beutenberg Str. 11, 07743 Jena, Germany

[b] Leibniz Institute for Zoo and Wildlife Research, Alfred-Kowalke-Straße 17, 10315 Berlin, Germany

[c] Institute of Medical Systems Biology, Ulm University, James-Franck-Ring, 89069 Ulm, Germany

1 authors contributed equally to this work

2 shared senior authors

Corresponding Author:

Martin Bens (martin.bens@leibniz-fli.de)

Keywords:

reproduction, sexual maturation, aging, RNA-seq, naked-mole rat, eusociality

Abstract

Naked mole-rats (NMRs) are eusocially organized in colonies. Although breeders carry the additional metabolic load of reproduction, they are extremely long-lived and remain fertile throughout their lifespan. Comparative transcriptome analysis of ten organs from breeders and non-breeders of the eusocial long-lived NMR and the polygynous shorter-lived guinea pig provide comprehensive and unbiased molecular evidence that sexual maturation in NMR is socially suppressed. After transition into breeders, transcriptomes are markedly sex-specific, show pronounced feedback signaling via gonadal steroids and have similarities to reproductive phenotypes in African cichlid fish. Further, NMRs show functional enrichment of status-related expression differences associated with aging. Lipid metabolism and oxidative phosphorylation – molecular networks known to be linked to aging – were identified among most affected gene sets. Further, a transcriptome pattern associated with longevity is reinforced in NMR breeders contradicting the disposable soma theory of aging and potentially contributing to their exceptional long life- and healthspan.

Introduction

The naked mole-rat (NMR, *Heterocephalus glaber*) has become increasingly popular as an animal model in a variety of research fields due to its unique biology. This includes an exceptionally long lifespan and resistance to cancer [1, 2]. According to The Animal Ageing and Longevity Database (AnAge) [3] the maximum recorded lifespan is 31 years, i.e. 368% of the prediction based on body mass. NMRs stay fertile throughout their long and healthy life, i.e. show an extraordinary long life- and healthspan [4]. This lifelong fertility becomes even more astonishing, considering the extreme reproductive skew in NMR colonies. Like eusocial insects, NMRs are socially organized in colonies consisting of a pair of reproducing animals (breeders, queen and pasha) and up to 300 subordinates (non-breeders, female and male workers) [5]. However, although workers are in principle capable of reproduction [6, 7], sexual maturation is suppressed through the behavior of the dominating queen [8]. Non-breeding animals of both sexes are the backbone of the social organization of the colony and take care of foraging, brood care, colony defense and digging [9].

Naturally, new NMR colonies originate from fissioning of existing colonies or formation of new ones by dispersers that leave their natal colony [10, 11]. When under laboratory conditions non-breeders are removed from the colony and paired with the opposite sex, they have the capability to ascend into breeders. This process is accompanied with physiological and behavioral changes, and results in the formation of a new colony [5, 6]. Remarkably, despite the queen's enormous metabolic load of producing a large litter every three months and being exclusively in charge of lactation [12], data from wild and laboratory NMR colonies indicate that breeders live longer than their non-breeding counterparts [13, 14]. This contrasts the disposable soma theory of aging, which hypothesizes that energy is either allocated to body maintenance or reproduction [15].

71 In NMR, the reproductive suppression in female non-breeders is mediated through inhibition
72 of gonadotropin-releasing hormone (GnRH) secretion from the hypothalamus [6]. This in
73 turn leads to an inhibition of follicle stimulating hormone (FSH) and luteinizing hormone
74 (LH) released by the pituitary gland and causes a block of ovulation. Also for male non-
75 breeders, reproductive suppression is caused by inhibition of GnRH secretion, which results
76 in lower levels of urinary testosterone and plasma LH [7]. The impact, however, is less
77 profound compared to females as spermatogenesis is attenuated, but not entirely suppressed
78 [16]. Nevertheless, weight of testis and number of active spermatozoa is higher in breeders [7,
79 17]. The role of GnRH in mediating environmental cues to allow or block reproduction is well
80 described in a variety of species [18, 19].

81 The NMR can be regarded as a neotenic species and the prolonged retention of juvenile
82 features has been linked to its longevity [20]. In comparison to mice, e.g. postnatal NMR brain
83 maturation occurs at slower rate [12] and puberty is delayed. Female and male NMRs may
84 reach sexual maturity at 7.5 to 12 months of age [21]. In the colony, however, the queen
85 suppresses sexual maturation in both non-breeding males and females by aggressive social
86 behavior [8] and can delay – independently of neoteny - the puberty of female workers for life
87 [22]. Thus, sexual dimorphism is almost absent among non-breeding NMRs [23, 24]. Both
88 sexes show almost no difference in morphology, including body mass, body size and even
89 external genitalia, as well as no behavioral differences, in the sense that non-breeders
90 participate and behave equally in all colony labors [25]. Nevertheless, these features are
91 correlated with colony rank. Most profound differences can be observed comparing NMR
92 queens vs. non-breeders, reflected in morphological differences, such as an elongated spine
93 and higher body mass of queens, as well as behavioral differences, such as increased
94 aggressiveness, copulation and genital nuzzling [25].

95 In this work, we characterized the transcript signature of reproductive status (breeder vs.
96 non-breeder) in tissue samples of ten organs or their substructures (hereinafter called for
97 simplicity "tissues") from both sexes using RNA-seq. We contrast the NMR results with the
98 transcript profiles of corresponding samples of guinea pig (GP, *Cavia porcellus*), a closely
99 related, polygynous, not long-lived rodent species (AnAge: 12 years maximal longevity, 89%
100 of the prediction based on body mass). We specifically focused our analyses on transcriptome
101 signatures of the socially-suppressed sexual maturation in NMR as well as on differentially
102 expressed genes (DEGs) that may contribute to the exceptional long life- and healthspan of
103 NMR breeders.

104

105 **Results**

106 To gain molecular insights into the fascinating combination of NMR phenotypes, in particular
107 their eusocial reproduction, lifelong fertility, extraordinary healthspan and longevity, we
108 aimed to collect a comprehensive set of tissue samples for male and female breeders and non-
109 breeders of NMR and GP - six biological replicates each. Towards this, NMR non-breeders
110 were removed from their natal colony, paired with an unrelated animal of the opposite sex
111 from a second colony and thereby turned into breeders. Respective male and female litter
112 siblings remained in the two colonies as non-breeder controls. Time to first litters averaged in
113 6.5±4.9 (±SD) months and duration of pregnancies was approximately 70 days. GP breeders
114 and non-breeders were housed as pairs of opposite or same sex, respectively. For this species,
115 the time to first litters was 4.1±0.8 month and the pregnancies lasted about 68 days.

116 Female breeders gave birth to two litters each, with two exceptions. One NMR female was
117 pregnant at least twice (ultrasonographically verified), but never gave birth to live offspring,
118 and another gave birth to three litters, due to a pregnancy fathered by one of her sons. At

119 time of sampling, NMRs and GPs reached an age of 3.4±0.5 and 0.9±0.1 years, respectively
120 (Table S1).

121

122 **Tissue and species are the major determinants of transcriptomes**

123 To compare gene expression between reproductive statuses (breeder vs. non-breeder) in
124 NMR and GP, we performed RNA-seq of ten different tissue samples (heart - Hrt, skin - Skn,
125 liver - Lvr, kidney - Kid, cerebellum - Cer, hypothalamus - Hyp, pituitary - Pit, thyroid - Thy,
126 adrenal - Adr, and gonads – Gon, represented by either ovary – Ova or testis – Tes) from
127 24 animals for each species (six males, six females per status; Fig. S1). Seven of the 480
128 samples (1.5%) had to be excluded for different reasons (Tables S2, S3). On average (±SD), we
129 obtained per sample 27.6±3.6 million high-quality reads with 84.1±16.1% unique mapping rate
130 (Table S4). The grand mean of pairwise Pearson correlation within the 40 replicate groups (2
131 statuses x 2 sexes x 10 tissues per sex) was 0.981±0.013 and 0.984±0.01 for NMR and GP,
132 respectively, indicating high consistency between replicate samples (Table S5).

133 Based on these data, unsupervised hierarchical clustering gave a similar cluster hierarchy of
134 tissues for both species (Fig. S2). Brain tissues are grouped (Pit as a sister group to Cer and
135 Hyp); Kid and Thy are sister groups to the cluster of Adr and Ova. The results are confirmed
136 by principle component analysis, separating tissues by the first and species by the second
137 component (Figure 1). At this level of analysis, ovary was the only tissue, which showed a
138 separation of samples with respect to breeding status. Together, this indicates that: (i) tissue
139 source is dominant over other biological variables such as species, sex and status and (ii) the
140 impact of sex and status on transcriptome profiles is subtle.

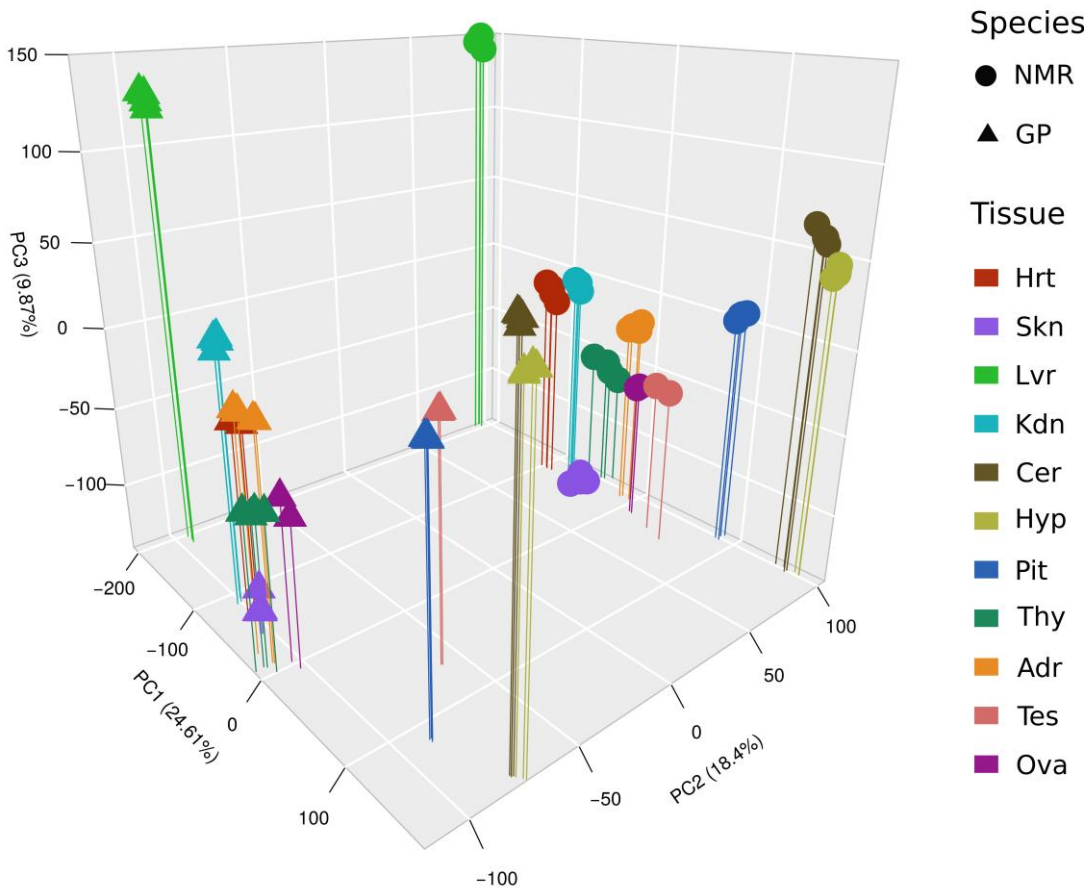

Figure 1: Principle component (PC) analysis of groups based on mean expression levels (four groups per tissue and species: 2 sexes x 2 statuses, except gonads). Tissues are separated by PC1 and PC3, species by PC2.

Cross-species DEGs are enriched in aging-related genes

To further characterize the species differences between the long-lived NMR and the shorter-lived GP, we determined gene expression differences based on orthologous transcribed regions that show high sequence similarity. This filtering method avoided potentially misleading signals that may arise from assembly artifacts or the comparison of different transcript isoforms and identified 10,127 genes suitable for further analyses.

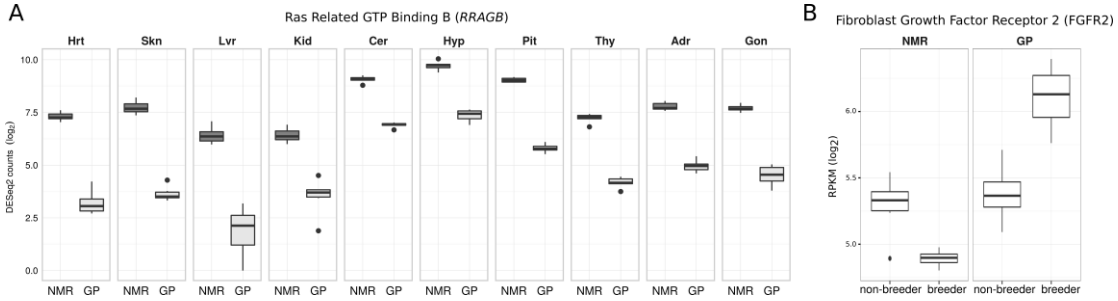

Figure 2: (A) Ras Related GTP Binding B (RRAGB) is consistently differentially expressed between species across all tissues. RRAGB is known to interact with mTORC1 complex [26, 27]. **(B)** Fibroblast Growth Factor Receptor 2 (FGFR2) shows opposing direction of expression between NMR and GP in breeders vs. non-breeders.

Across all tissues, we identified 18,000 significant expression differences (EDs; 9,651/8,349 higher/lower expressed in NMR) in 5,951 out of 10,127 genes (FDR<0.01, $|\log_2 FC|>2$; Table S6, Supplemental Data S1-S11). Among genes that are consistently differentially expressed across all tissues, we identified aging-related candidates. E.g. *RRAGB* (Ras related GTP binding B, Figure 2A) and *TMEM8C* (transmembrane protein 8C) are higher expressed in NMRs. *RRAGB* interacts with mTORC1 complex [26, 27]. *TMEM8C* is essential for muscle regeneration [28] and might be linked to the resistance to muscle loss in aged NMRs [29, 30].

To further assess the association of cross-species DEGs with aging, we examined their overlap with aging-related genes of human and mouse obtained from the Digital Ageing Atlas (DAA) [31]. This test revealed a significant overlap with DAA containing 1,056 genes (17.74% of DEGs; p=0.006, Fisher's exact test (FET); Table S7). The enrichment analysis of shared aging-related genes (Table S8) reveals that the top ranked GO term set is associated with lipid biosynthetic process (GO:0008610) (Fig. S3), a finding referring to existing links between lipid metabolism and lifespan [32, 33].

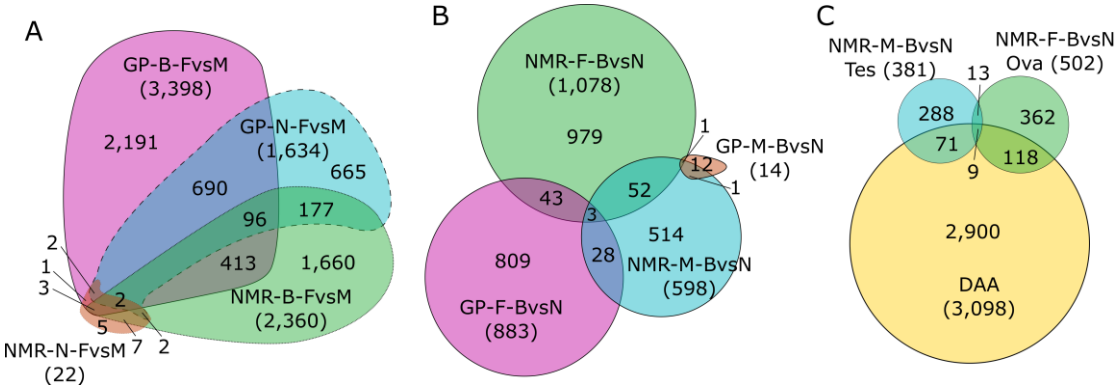

Figure 3: Euler diagrams showing overlaps of DEGs. **(A)** Female vs. male. **(B)** Breeder vs. non-breeder. **(C)** Gonads of NMR breeder vs. non-breeder and aging-related genes from the Digital Aging Atlas (DAA).

Sexual differentiation and maturation in NMR are delayed until transition from worker to breeder

The DEGs between sexes were determined within the groups of non-breeders and breeders for each tissue and species (Table 1, Table S9, Supplemental Data S12-S47). GP non-breeder females vs. males (GP-N-FvM) show over all tissues except gonads 1,713 significant expression differences (EDs) in 1,634 genes (FDR<0.01, Table 1), primarily in Adr (858 DEGs), Lvr (383), Thy (347) and Kid (109). Between female and male GP breeders (GP-B-FvM) 3,654/3,398 EDs/DEGs were observed. These transcriptome data confirm a clear sexual differentiation among sexually mature GPs that further increases after onset of breeding. Breeders have 790 DEGs in common with non-breeders ($p<2.2x10^{-16}$, FET; Figure 3A). Functional enrichment analysis of these shared genes reveals among the highest ranked GO sets immune system related terms (Fig. S5, Table S10).

192 **Table 1:** Numbers of DEGS identified in the different comparisons (FDR<0.01).

	female vs. male				breeder vs. non-breeder			
	non-breeder		breeder		females		males	
Tissue	GP	NMR	GP	NMR	GP	NMR	GP	NMR
Hrt	4	10	89	13	2	3	0	0
Skn	6	6	3	5	5	1	0	223
Lvr	383	4	235	10	71	0	9	1
Kid	109	6	106	21	1	4	0	0
Cer	1	5	2	25	0	15	0	0
Hyp	2	8	1	11	0	5	2	0
Pit	347	9	307	47	114	114	2	1
Thy	3	0	2,087	1,791	675	285	1	0
Adr	858	4	824	533	0	201	1	4
Gon	-	-	-	-	18	502	3	381
ED*	1,713	52	3,654	2,456	886	1,130	18	610
NR†	1,634	22	3,398	2,360	883	1,078	14	598

193

194 * significant expression differences across tissues

195 † non-redundant set of significant expression differences across tissues

196

197 Similarly to GP-B-FvM, NMR-B-FvM showed 2,456/2,360 sex-related EDs/DEGs (FDR<0.01),
198 mostly in Thy (1,791) and Adr (533). The overlap with GP-B-FvM is with 514 DEGs
199 considerable but does not reach significance (p=0.062, FET; Figure 3A). Nevertheless, these
200 data indicate basic similarities in sexual differentiation among breeders of both species.

201 Surprisingly, only 22 NMR-N-FvM EDs/DEGs were detected across all tissues (Table S11),
202 indicating an only minor sex differentiation between NMR non-breeding females and males
203 on the transcriptional level, consistent with the almost absent sexual dimorphism among non-
204 breeding NMRs [23, 24].

205

206 **Status change of NMRs is accompanied by major changes in the endocrine system**

207 The DEGs between breeders and non-breeders were determined within the same sex for each
208 species (Table 1; Table S12, Supplemental Data S48-S87). Females showed a similar amount of
209 EDs/DEGs in both species (GP-F-BvN: 886/883, NMR-F-BvN: 1,130/1,078) but have only 46
210 DEGs in common (Figure 3B). This is less than expected by chance, although not reaching
211 significance (p=0.075, FET for depletion) and indicates that the molecular signature of the
212 transition from female non-breeder to breeder is different in both species. E.g. in GP-F-BvN,
213 only 18 DEGs are observed in Ova and none in Adr while in NMR-F-BvN, these tissues show
214 most of the differences with 502 and 201 DEGs, respectively. Functional enrichment analysis
215 of DEGs in NMR Ova identifies reproductive structure development (GO:0048608) as the
216 highest ranked category (Fig. S6, Table S13). The same analysis in Adr revealed an obvious
217 directionality in expression changes. DEGs are preferentially upregulated among highest
218 ranked GO term sets (Fig. S7, Table S14), e.g. in reproduction (GO:0000003, 24 of 28) and
219 endocrine system development (GO:0035270, 17 of 18). Tallying with this, Cer DEGs are
220 enriched and upregulated in steroid metabolic process (GO:0008202, 6 of 6 upregulated) and
221 response to hormones (GO:0009725, 7 of 7) (Fig. S8, Table S15).

222 In male GPs, status-related differences (GP-M-BvN) were almost absent across all tissues
223 (only 18 EDs/14 DEGs). In contrast, NMR-M-BvN showed 610/598 EDs/DEGs, predominantly
224 in Tes (381) and Skn (223). NMRs share 55 status-related DEGs in both sexes (p=0.008, FET;
225 Table S16), while the few status-related changes in male GPs showed no overlap with those in
226 females (Figure 3B). Among shared DEGs in NMRs, 10 genes involved in endocrine signaling
227 were identified, including *SSTR3* (somatostatin receptor), *TAC4* (tachykinin), *PRDX1*
228 (peroxiredoxin 1) and ACPP (acid phosphatase, prostate), as well as in general signaling via
229 cAMP signaling (three genes) and through G-protein coupled receptors (four genes) further

230 underlining that social status transition in NMR is associated with changes in the endocrine
231 system.

232

233 **Mitochondrial genes show opposed expression changes in Tes and Skn after status change**
234 **of NMR males**

235 In NMR-M-BvN Tes, functional enrichment analysis revealed as highest ranked metabolism-
236 and energy-related GO sets. DEGs enriched therein are mostly upregulated, e.g. lipid
237 biosynthetic process (GO:0008610, 75 of 82 genes) and oxidation-reduction process
238 (GO:0055114, 64 of 64) (Fig. S9, Table S17). Furthermore, we observed an upregulation of
239 response to stimulus (GO:0050896, 79 of 106), in line with an upregulation of steroid
240 metabolic process (GO:0008202, 28 of 28) included in lipid biosynthetic process set. In
241 accordance with the dominance of energy-related processes, DEGs are enriched and
242 preferentially upregulated in the top GO cellular component terms mitochondria
243 (GO:0005739, 61 of 62) and peroxisomes (GO:0005777, 13 of 13) (Table S18). Together, this
244 indicates increased demands of energy, e.g. to produce steroid hormones in Tes of NMR
245 breeders.

246 Similar to Tes, Skn showed enrichment of energy-related processes (Table S19, Fig. S10).
247 However, GO term sets in Skn are mostly downregulated, including energy derivation by
248 organic compounds (GO:0015980, 36 of 38 genes) and oxidation-reduction process
249 (GO:0055114, 42 of 46). Consistently, this includes genes associated with mitochondria
250 (GO:0044429, 56 of 57) and respiratory chain (GO:0070469, 11 of 11).

251

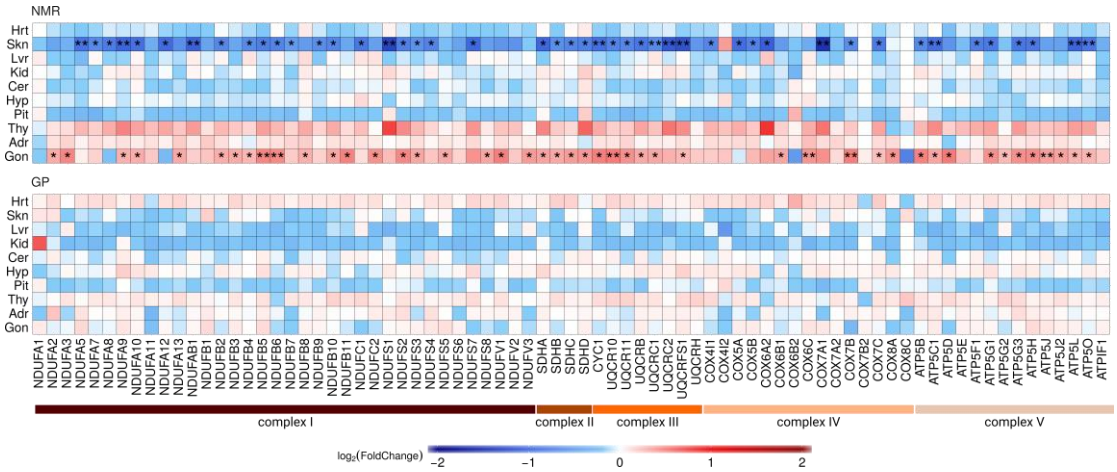

Figure 4: Expression changes of nuclear genes encoding for mitochondrial respiratory chain complexes in status change of male NMRs (top) and GPs (bottom). DEGs are indicated by asterisk (*: FDR<0.05, **: FDR<0.01). Only NMRs show significant expression differences (skn: 46 genes, mean fold-change 0.76; tes 46 genes, mean fold-change 1.89).

The overlap between mitochondrial DEGs in Tes and Skn comprises 6 genes ($p=7.27 \times 10^{-8}$, FET; Figure 4). Among common genes *PINK1* (PTEN induced putative kinase 1) is 1.5-fold upregulated in Tes and 2.5-fold downregulated in Skn, indicating a role in regulation of mitophagy [34] in both tissues.

To follow up the mitochondria-related findings, the 'mitonuclear transcript ratio' was determined as the read count ratio of mitochondrial-encoded genes versus nuclear-encoded genes. It differs largely between tissues and species (Table S20). Hrt showed the highest mitonuclear ratio, with a minor difference between species (NMR 30.1%, GP 30.4%). Tes showed the lowest ratio, particularly in GPs (NMR 5.5%, GP 0.9%), and a 43.1% increase in NMR-M-BvN (Fig. S11). This increase is accompanied with an upregulation of nuclear genes encoding for mitochondrial respiratory chain complexes (Figure 4; Table S21). The expected increase in ROS is compensated by an on average 1.59-fold upregulation of eight antioxidant

270 DEGs (Table S22). Consistently with functional enrichment analysis mentioned above, an
271 opposing effect in Skn of NMR male breeders was observed, which showed a decline in
272 mitonuclear ratio together with a downregulation of nuclear genes of the respiratory
273 complexes (Figure 4). In line with the downregulation of the oxidative phosphorylation
274 pathway (OXPHOS), a downregulation of antioxidant enzymes SOD2 (superoxide dismutase
275 2, 2.64-fold) and PRDX3 (peroxiredoxin 3, 2.14-fold) was observed. In general,
276 downregulation of OXPHOS is linked to an extended lifespan [32, 35–37].

277

278 **NMR status-related DEGs are enriched in aging-related genes**

279 Guided by the exceptional long life- and healthspan of NMR breeders, we searched our
280 transcriptome data for molecular signatures relating to this phenomenon. First, we found that
281 only NMRs show status-related DEGs that are significantly enriched for aging-related genes
282 from DAA (Table S23): males in Skn (55 genes; q=0.0012, FET) and Tes (80 genes, q=0.01), and
283 females in Ova (127 genes; $q=1.2x10^{-7}$), Thy (59 genes, q=0.033) and Adr (43 genes, q=0.038).
284 The significant overlap of 22 DEGs between NMR-F-BvN and NMR-M-BvN in Gon (p=0.0035,
285 FET) contains nine aging-related genes (p=0.004, Figure 3C). In GP, only the non-redundant
286 set of DEGs in GP-F-BvN showed a tendency of enrichment (160 genes, q=0.051), in contrast
287 to NMRs, which showed enrichment in males (134 genes, $q=4.5x10^{-5}$) and females (245 genes,
288 $q=7x10^{-9}$).

289 Second, we hypothesized that reproduction impacts the life expectancy of NMR and GP
290 differently. Therefore, we searched for status-related DEGs that are shared in both species,
291 but show opposing direction of expression. These genes might mark different coping
292 mechanisms with the metabolic load of reproduction. As described above, the overlap of
293 DEGs between species is very low (Table S24). Nevertheless, opposing direction of expression

294 change can be observed in Ova (1 of 2 shared DEGs), and female thyroid (8/8) and testis (1/1).
295 E.g. the fibroblast growth factor receptor 2 gene (*FGFR2*), linked to aging (AgeFactDB) [38], is
296 in Ova downregulated in NMRs, but upregulated in GPs (Figure 2B).

297 Third, and based on the assumption that status-related EDs with the greatest interspecies
298 difference (regardless of directionality) have an impact also on species-specific aging
299 trajectories of breeders, we determined enrichment of aging-related genes in the upper
300 quintile of those genes (Table S25). In males, we found significant enrichments of DAA genes
301 in Skn ($q=7.04x10^{-7}$) and Tes (q=0.0025); in females in Skn (q=0.0064), Hrt (q=0.0024), Pit
302 (q=0.0053) and Ova (q=0.0013). Further functional enrichment analysis of these aging-related
303 gene sets reveals differences between sexes. In males, the non-redundant set of genes shows
304 enrichment for lipid metabolism (GO:0006629), energy metabolism (energy derivation by
305 oxidation of organic compounds, GO:0015980; mitochondrial ATP synthesis coupled proton
306 transport, GO:0042776), glutathione metabolic process (GO:0006749) and immune system
307 (innate immune response-activating signal transduction, GO:0002758) (Table S26, Fig. S12).
308 Females showed enrichment in positive regulation of tumor necrosis factor production
309 (GO:0032760) and negative regulation of programmed cell death (GO:0043069) (Fig. S13,
310 Table S27).

311

312 **Status related changes in NMR contradict the disposable some theory**

313 Moreover, we assessed the connection of cross-species DEGs with expression changes that are
314 associated with status change in each species. Based on DEGs shared in two comparisons
315 (NMR vs. GP and breeder vs. non-breeder, FDR<0.05), we performed a correlation analyses of
316 fold changes in each species. We hypothesized – in agreement with the disposable soma
317 theory of aging – a negative impact of reproduction on lifespan for GP and – in contradiction

318 to this theory – an inverse effect for NMR. This was confirmed by opposing correlations
319 (combined $p=4.2x10^{-9}$ (Lancaster procedure [39]), negative correlation for GP and positive
320 correlation for NMR (Figure 5). This means that DEGs with higher expression in NMR than
321 GP are preferentially upregulated in NMR breeders compared to non-breeders, and vice
322 versa; in other words, a transcriptome pattern associated with longevity (NMR vs. GP) is
323 reinforced by the status transition (breeder vs. non-breeder) and thus may contribute to the
324 exceptional long life- and healthspan of NMR breeders.

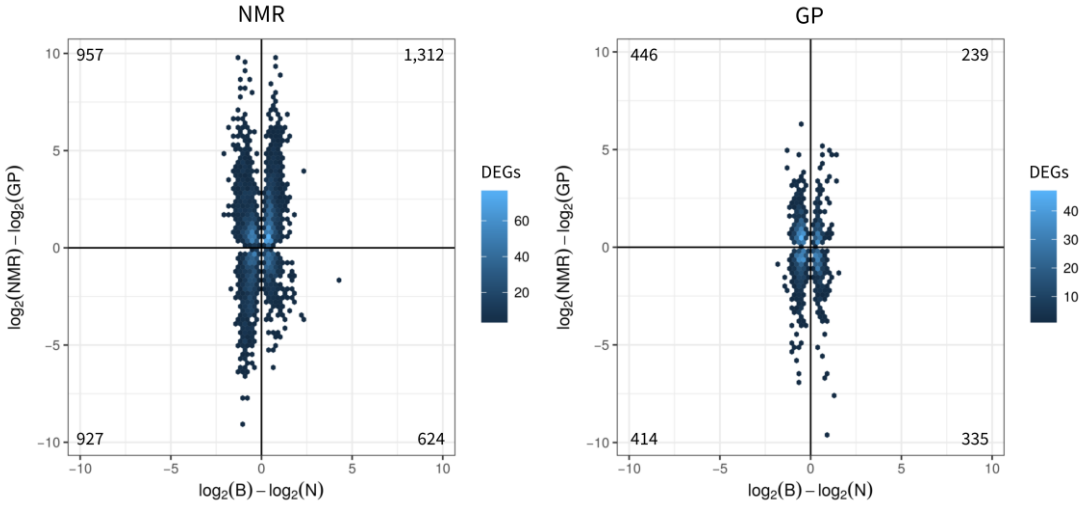

325

326 **Figure 5**: DEGs (FDR<0.05) occurring in both comparisons: cross-species (NMR vs. GP, y-
327 axes) and status change GPs (breeder vs. non-breeder, x-axes) separately for (A) NMRs and
328 (B). Correlation analysis between species shows opposing correlation (Lancaster procedure
329 [39], $p=4.2x10^{-9}$), while status-related DEGs in NMR are positively correlated with cross-
330 species DEGs (DEGs=3,820; spearman correlation=0.17, $p=3.2\times10^{-27}$), status-related DEGs in
331 GP show a negative correlation (1,434; -0.1; 1.8×10^{-4}).

332

333 ## Discussion

334 In our comparative study of breeders vs. non-breeders of the eusocial long-lived NMR and
335 the polygynous and shorter-lived GP, we accumulated a comprehensive set of transcriptome

336 data to gain insights into molecular networks underlying naturally evolved interspecies
337 differences in sexual maturation and links between reproduction and aging. Both species are
338 able to breed year-round and produce four to five litters per year [40, 41]. Both species have a
339 similar average gestation period of 70 days, which is long compared to similarly sized
340 species. Notably, NMRs produce on average 10.5 offspring per litter, which is twice the
341 number of offspring produced by similarly sized rodents and more than three times higher
342 compared to GPs (average 3.2 offspring) [40, 41]. This underscores the apparent contradiction
343 of the NMR queen's enormous metabolic load and extraordinary long life- and healthspan [4]
344 to the disposable soma theory of aging [15], indicating that natural ways to extended
345 healthspan remains to be uncovered in NMRs.

346 A first study to identify adaptations to unique NMR traits at the transcriptome level
347 compared liver gene expression of young adult non-breeding male NMRs and mice [42].
348 Higher NMR transcript levels were observed for genes associated with oxidoreduction and
349 mitochondria. This present study, more comprehensive in several aspects (sex, breeding
350 status, numbers of animals and tissue samples), is based on a comparison of NMR vs. GP,
351 which are phylogenetically closer than NMR and mouse. It revealed that between NMR and
352 GP 58.8% of the analyzed genes are differentially expressed and that these DEGs are
353 significantly enriched for aging-related genes. Among the latter, the main functional
354 commonality is their association with lipid metabolism. Links of this molecular network to
355 longevity of NMR were also obtained by a parallel proteome comparison of NMR and GP
356 livers [43]. This study also shows that NMR liver mitochondria exhibit an increased capacity
357 to utilize fatty acids.

358 In respect to sex-specific molecular signatures among either breeders or non-breeders in
359 NMR and GP, the main finding is a nearly complete absence of significant transcriptional

360 differences between sexes in non-breeding NMRs. This fits their grossly identical morphology
361 and identical behavior in stable colonies [25]. This is in stark contrast to non-breeding GPs of
362 an even younger age where we observed more than a thousand DEGs. GP non-breeders and
363 breeders share a large and highly significant number of sex-related DEGs. Among others,
364 these DEGs are enriched in GO terms related to steroid metabolism and immune system. The
365 effect of gonadal steroids on the immune system is well described in GPs and other mammals
366 [44]. After separation of NMR non-breeders from their colony, sexes became not only
367 distinguishable by morphology and behaviour [22, 25], but also by gene expression. This
368 differentiation on transcriptional level provides further molecular support for the previously
369 described suppression of sexual maturation in non-breeding adult NMRs by social stress [8,
370 22] and identified major changes in the endocrine system after status change in NMRs but not
371 in GPs (Supplement Text S1). Notably, we found no significant differences in gonadotropin-
372 related genes (Supplement Text S2), indicating similar transcript turnovers in both non-
373 breeders and breeders, and in line with previous results indicating that LH is stored in non-
374 breeders, ready to be released upon GnRH signalling [45].

375 Glucocorticoids have been linked to stress, reproduction and social behavior in a variety of
376 species, including members of muroidae, primates and cichlids [46–48]. In NMRs, however,
377 correlation between social status and urinary cortisol is not clear and seems to depend on
378 colony stability [49, 50]. Here, we observed a significant upregulation of *NR3C1*
379 (glucocorticoid receptor) in Tes of NMR male and Thy of female breeders (Supplemental
380 Data S55/67). Interestingly, this is in line with elevated expression of glucocorticoid receptor
381 in Tes in African cichlid breeders. Males can reversibly change between dominant and
382 subordinate phenotypes [51]. Similar to NMRs, only dominant phenotypes are reproductively
383 active. In male African cichlids, moreover, aggression is negatively correlated with expression
384 of *SSTR3* (somatostatin receptor 3) in Tes. Similarly, we observed in NMR breeder Tes

385 significant downregulation of *SSTR3* (Supplemental Data S67). This indicates that *SSTR3* may
386 be associated with social dominance in NMRs as well.

387 As our study was primarily motivated by the exceptional long life- and healthspan of NMR
388 breeders, we searched for evidence indicating that NMR status change has an impact on
389 genes involved in aging. We found enrichment of aging-related genes in the non-redundant
390 DEG sets of males and females, as well as enrichment in most tissues with at least 50 DEGs
391 (male Skn and Tes; female Ova, Thy and Adr). This contrasts with our observations in GPs,
392 which showed only a tendency of aging-relation for the non-redundant set of status-related
393 DEGs in females.

394 Further, we observed significant tissue-specific changes in OXPHOS of male NMR breeders.
395 While Tes showed an upregulation of nuclear-encoded mitochondrial genes and a respective
396 increase in mitonuclear transcript ratio, Skn showed the opposite. Moreover, we observed
397 significant enrichments of genes involved in fatty acid metabolism among status-related
398 DEGs in both NMR tissues. Consistent with the role of mitochondria in lipid homeostasis and
399 the observed directionality of changes in OXPHOS, fatty acid metabolism DEGs in Tes were
400 preferentially up- and in Skn downregulated. While the increased mitochondrial activity in
401 Tes probably complies with demands of energy for the production of sex steroids and their
402 anabolic effect on physiology, such as growth of testis [17], the observed changes in Skn may
403 indicate a link to the extraordinary healthspan of NMR breeders. Previously, it was observed
404 that inhibition of complex I activity during adult life prolongs lifespan and rejuvenates the
405 tailfin transcriptome in short-lived fish [36]. Enhanced lipid metabolism and reduced
406 mitochondrial respiration were also linked to NMR longevity in a parallel liver proteome
407 study comparing NMR vs. GP and old vs. young NMR [43].

408 Finally, we performed a correlation analysis between species (NMR vs. GP) and status
409 (breeder vs. non-breeder) EDs confirming the basic hypothesis of the present work: in
410 contrast to GP and in line with recent demographic studies performed in NMRs [14], the
411 transition into breeders results in molecular signatures linked to extended life- and
412 healthspan only in NMRs. Genes which are higher or lower expressed in NMR compared to
413 GP are also preferentially up- or downregulated in NMR breeders (positive correlation)
414 opposite to GPs (negative correlation). In other words, the positive correlation in NMR
415 contradicts the disposable soma theory of aging, as EDs contributing to a long lifespan
416 (higher/lower expression in NMR than GP) are preferentially increased in NMR breeders
417 compared to non-breeders, while diminished in GPs as expected by this theory.

418 Taken together, our comparative transcriptome analysis of breeders versus non-breeders of
419 the eusocial, long-lived NMR versus the polygynous and shorter-lived GP identifies
420 molecular networks underlying socially regulated sexual maturation and naturally evolved
421 extended life- and healthspan that encourage further functional and mechanistic
422 investigations of these extraordinary NMR phenotypes.

423

424 ## Materials & Methods

425 ### Animals

426 *Naked mole-rats.* NMR colonies were kept inside a climatized box (2x1x1 m) in artificial
427 burrow systems, consisting of eight cylindrical acrylic glass containers (diameter: 240 mm
428 height: 285 or 205 mm). The latter functioned as variable nest boxes, food chambers or toilet
429 areas, and were interconnected with acrylic tubes having an inner diameter of 60 mm.
430 Husbandry conditions were stabile during the entire experimental period of 22 months.
431 Temperature and humidity were adjusted to 27.0±2.0°C and 85.0±5.0%, respectively. In

432 general, the NMR colonies were kept in darkness except for 2 to 4 hours of daily husbandry
433 activities. Fresh vegetable food was provided daily and *ad libitum*. In addition, commercial rat
434 pellets (Vita special, Vitakraft GmbH, Bremen, Germany) were fed as an additional source of
435 protein and trace elements.

436 To turn them into breeders, randomly selected non-breeding animals derived from two long-
437 term (>4 years) established colonies of more than 50 individuals were separated and paired
438 with the opposite sex. As non-breeder controls, litter siblings of paired animals remained in
439 their colonies as workers. After the lactation period of the second set of live offspring the
440 tissue sampling was scheduled. To avoid further pregnancies in the females, male partners
441 were removed and euthanized 8-10 days postpartum. The tissue collection in the females took
442 place 40-50 days after the end of last pregnancy.

443 *Guinea pigs*. GPs (breed: Dunkin Hartley HsdDhl:DH, Harlan Laboratories, AN Venray,
444 Netherlands) were housed in standardized GP cages (length: 850 mm, width: 470 mm, height:
445 450 mm) in breeding pairs plus offspring or in same-gender pairs of two. Commercial guinea
446 pig pellets and commercial pet food hay (Hellweg Zooland GmbH, Berlin, Germany) were
447 provided together with vitamin C enriched water *ad libitum*. Housing temperature and
448 humidity were 18.0±2.0°C and 45.0±5.0%, respectively. A 12h light/dark regime was provided.

449 After an initial adaption period of 6 to 8 weeks the GPs were randomly divided in breeding
450 pairs or in same-gender pairs of two. The offspring were separated from their parents after
451 weaning (~3 weeks postpartum). Tissue collection was scheduled after the lactation period of
452 the second set of live offspring. To avoid further pregnancies in the females, male partners
453 were removed between eleven days before and seven days after birth of the second litter. The
454 tissue collection in the females took place 42-83 days after the end of last pregnancy.

455 For tissue collection, all animals were anaesthetized by 3% isoflurane inhalation anaesthesia
456 (Isofluran CP, CP-Pharma, Burgdorf, Germany) and euthanized by surgical decapitation.
457 Animal housing and tissue collection at the Leibniz Institute for Zoo and Wildlife Research
458 was compliant with national and state legislation (breeding allowance #ZH 156; ethics
459 approval G 0221/12 "Exploring long health span", Landesamt für Gesundheit und Soziales,
460 Berlin).

461

462 **Sample collection, RNA Isolation and Sequencing**

463 For *de novo* transcriptome assembly, animals were euthanized and ten tissue samples (heart –
464 Hrt (NMR only), skin - Skn, liver - Lvr, kidney - Kid, cerebellum - Cer, hypothalamus - Hyp,
465 pituitary - Pit, thyroid - Thy, adrenal - Adr, and gonads - Gon (testis – Tes /ovaries - Ova))
466 were collected from NMR and GP individuals, as described previously [52]. Strand-specific
467 RNA-seq were prepared using the TruSeq Stranded RNA LT Kit (Illumina), and 200-nt reads
468 were obtained using a HiSeq2500 (Illumina), as described previously [52].

469 For expression analysis, the same ten tissues were collected from NMR and GP breeders and
470 non-breeders. RNA was purified as described above. Library preparation was done using
471 Illumina's TruSeq RNA Library Prep Kit v2 kit following the manufacturer's description.
472 Quantification and quality check of the libraries was done using Agilent's Bioanalyzer 2100 in
473 combination with a DNA 7500 Kit (both Agilent Technologies). Sequencing was done on a
474 HiSeq 2500 running the machine in 51 cycle, single-end, high-output mode by multiplexing
475 seven samples per lane. Demultiplexing and extraction of read information in FastQ format
476 was done using the tool bcl2astq v1.8.4 (provided by Illumina).

477

478 **Data Analysis**

479 *De novo* transcriptome assembly and annotation for GP was performed as described in [52].
480 Briefly, overlapping paired-end reads were joined into single fragments and then assembled
481 by Trinity [53]. Gene symbols were assigned to the assembled transcripts by similarity to
482 human transcripts using FRAMA [52].

483 As a reference for RNA-seq data mapping the public NMR (Bioproject PRJNA72441) [54] and
484 GP genomes (UCSC, cavpor3) were used. Reference transcript sets of NMR and GP were
485 mapped to the corresponding genome in two steps: BLAT (v36) [55] was used to identify the
486 locus and then SPLIGN (v1.39.8) [56] was applied to splice align the transcript sequence
487 within BLAT locus. RNA-seq data were aligned to the corresponding reference genome
488 utilizing STAR (v2.4.1d) [57] with a maximum mismatch of 6% and a minimum aligned
489 length of 90%. Reads mapped to multiple loci were discarded. Gene expression was
490 quantified using HTSEQ (v0.6.1p1) [58] based on the aligned reference transcripts. The
491 pairwise Pearson correlation between biological replicates was calculated based on 16,339 and
492 16,009 genes in NMR and GP, respectively (Table S5).

493 The 'mitonuclear transcript ratio' was calculated as the read count ratio of 13 mitochondrial-
494 encoded genes versus all nuclear-encoded genes.

495 PosiGene was applied to the transcriptome of human, NMR and GP with the parameter
496 '-prank=0 -max_anchor_gaps_hard=100 -rs=NMR' to determine orthologous transcribed
497 regions in NMR and GP having a protein identity >70%. RNA-seq data were aligned to the
498 corresponding transcriptomes utilizing bowtie2 (2.2.9) [59] with the parameter
499 '-very-sensitive-local'.

500 DESeq2 (v1.6.3) [60] was used to identify DEGs. A false discovery rate <0.01 (FDR; Benjamini
501 Hochberg corrected p values, [61]) was used for the identification of significant DEGs.

502 Gene Ontology analysis was performed using the web interface of GoMiner (Database build
503 2011-01) based on the functional annotation of human genes (UniProt) [62]. A FDR<0.05 was
504 used for the identification of significant GO terms that were summarized by REVIGO
505 (parameter SimRel=0.5) into non-redundant GO term sets [63]. GO term sets were then
506 ranked by number of summarized GO terms and number of changed genes. KEGG analysis
507 was performed using Fisher's exact test and significant pathways were identified using
508 FDR<0.05. KEGG results were redundant to Gene Ontology analysis and therefore not shown.

509 Overlap between gene sets was determined with Fisher's exact test (FET) using the one-sided
510 option. Generally, we tested for enrichment if not otherwise stated.

511 We obtained 3,009 aging-related genes in human and mouse from the Digital Ageing Atlas
512 (DAA) [31]. The corresponding counterparts in the NMR (2,588) and GP (2,539) were used for
513 enrichment analysis and results were corrected for multiple testing (FDR). P-values corrected
514 for multiple testing are indicated by q and nominal p-values by p.

515 To examine the connection between reproduction and aging in both species, we determined
516 the difference in log2-fold-change (breeders vs. non-breeders) of NMR and GP. For fold-
517 changes moving in opposite directions between species, we calculated the absolute difference
518 ($|\log_2 NMR_{BvsN} - \log_2 GP_{BvsN}|$), and for fold-changes moving in the same direction, higher
519 fold-changes in NMR-BvN were rewarded ($|\log_2 NMR_{BvsN}| - |\log_2 GP_{BvsN}|$). The 20%-
520 quantile of genes having the greatest difference was determined separately for (i) the
521 complete gene set and for genes showing (ii) opposing and (iii) unidirectional fold-changes.
522 All sets were tested for enrichment of aging-related genes.

523 Statistical analyses were performed in R (version v3.1.2).

524

525 **Data Availability**

526 RNA-seq data for gene expression profiling were deposited at Gene Expression Omnibus
527 (GSE98719). RNA-seq data for *de novo* assembly were deposited at Sequence Read Archive
528 (SRP104222, SRP061363) and the corresponding gene collection is available as a gff3-file
529 (ftp://genome.leibniz-fli.de/pub/nmr2017/).

530

531 ## Acknowledgements

532 We like to acknowledge Angelika Kissmann and Jette Ziep for their professional help with
533 the animal husbandry. We also thank Michaela Wetzel for her logistic help during tissue
534 sampling and storage as well as for her support with the animal husbandry. We are grateful
535 to Ivonne Görlich for excellent technical assistance as well as Debra Weih and Steve
536 Hoffmann for critical reading of the manuscript.

537

538 ## Funding

539 This research was supported by the Leibniz-Gemeinschaft through the
540 Senatsausschusswettbewerb (SAW), grant SAW-2012-FLI-2, and the Deutsche
541 Forschungsgemeinschaft (DFG), grant PL 173/8-1.

542

543 ## Competing interests

544 None declared.

545

Author Contributions

TBH, MP and KS conceived the project. SH, TBH, MB, MG and KS performed the animal study, sampling and sequencing experiments. Data analysis and interpretation were performed by MB, KS, SH, AS, HK, MP and TBH. The manuscript was written by MB and KS, and revised by all authors. The manuscript submitted by MB; all authors reviewed and approved the submitted manuscript. TBH and MP are joint senior authors.

Abbreviations

DEG	differentially expressed gene
ED	expression differences
FDR	false discovery rate
FET	Fisher's exact test
GO	Gene Ontology
GP	guinea pig
GP-B-FvM	comparison of GP Breeder Females vs. Males
GP-F-BvN	comparison of GP Female Breeders vs. Non-breeders
GP-M-BvN	comparison of GP Male Breeders vs. Non-breeders
GP-N-FvM	comparison of GP Non-breeder Females vs. Males
NMR	naked mole-rat
NMR-BvN	comparison of NMR Breeders vs. Non-breeders (both sexes)
NMR-B-FvM	comparison of NMR Breeder Females vs. Males
NMR-F-BvN	comparison of NMR Female Breeders vs. Non-breeders
NMR-M-BvN	comparison of NMR Male Breeders vs. Non-breeders
NMR-N-FvM	comparison of NMR Non-breeder Females vs. Males

References

1. Kim EB, Fang X, Fushan A a., Huang Z, Lobanov A V, Han L, et al. Genome sequencing reveals insights into physiology and longevity of the naked mole rat. Nature. 2011;479:223–7.

2. Tian X, Azpurua J, Hine C, Vaidya A, Myakishev-Rempel M, Ablaeva J, et al. High-molecular-mass hyaluronan mediates the cancer resistance of the naked mole rat. Nature. 2013;499:346–9. doi:10.1038/nature12234.

3. Tacutu R, Craig T, Budovsky A, Wuttke D, Lehmann G, Taranukha D, et al. Human Ageing Genomic Resources: Integrated databases and tools for the biology and genetics of ageing. Nucleic Acids Res. 2013;41:D1027–33. doi:10.1093/nar/gks1155.

4. Buffenstein R, Jarvis JUM. The naked mole rat--a new record for the oldest living rodent. Sci aging Knowl Environ. 2002;2002:pe7. doi:10.1126/sageke.2002.21.pe7.

5. Jarvis JU. Eusociality in a mammal: cooperative breeding in naked mole-rat colonies. Science. 1981;212:571–3. doi:10.1126/science.7209555.

6. Faulkes CG, Abbott DH, Jarvis JU. Social suppression of ovarian cyclicity in captive and wild colonies of naked mole-rats, Heterocephalus glaber. Reproduction. 1990;88:559–68. doi:10.1530/jrf.0.0880559.

7. Faulkes CG, Abbott DH, Jarvis JUM. Social suppression of reproduction in male naked mole-rats, Heterocephalus glaber. J Reprod Fertil. 1991;91:593–604. doi:10.1530/jrf.0.0910593.

8. Smith TE, Faulkes CG, Abbott DH. Combined olfactory contact with the parent colony and direct contact with nonbreeding animals does not maintain suppression of ovulation in female naked mole-rats (Heterocephalus glaber). Horm Behav. 1997;31:277–88. doi:10.1006/hbeh.1997.1384.

9. Burda H, Honeycutt RL, Begall S, Locker-Grutjen O, Scharff A. Are naked mole-rats eusocial and if so, why? Behav Ecol Sociobiol. 2000;47:293–303.

10. Braude S. Dispersal and new colony formation in wild naked mole-rats: evidence against inbreeding as the system of mating. Behav Ecol. 2000;11:7–12.

11. O'Riain MJ, Jarvis JU, Faulkes CG. A dispersive morph in the naked mole-rat. Nature. 1996;380:619–21.

599 12. Orr ME, Garbarino VR, Salinas A, Buffenstein R. Extended Postnatal Brain Development
600 in the Longest-Lived Rodent: Prolonged Maintenance of Neotenous Traits in the Naked Mole-
601 Rat Brain. Front Neurosci. 2016;10:504. doi:10.3389/fnins.2016.00504.
602 13. Hochberg ME, Noble RJ, Braude S. A Hypothesis to Explain Cancers in Confined Colonies
603 of Naked Mole Rats. bioRxiv. 2016.
604 14. Ruby JG, Smith M, Buffenstein R. Naked mole-rat mortality rates defy Gompertzian laws
605 by not increasing with age. Elife. 2018;7:e31157. doi:10.7554/eLife.31157.
606 15. Kirkwood TB. Evolution of ageing. Nature. 1977;270:301–4.
607 16. van der Horst G, Maree L, Kotzé SH, O'Riain MJ. Sperm structure and motility in the
608 eusocial naked mole-rat, Heterocephalus glaber: a case of degenerative orthogenesis in the
609 absence of sperm competition? BMC Evol Biol. 2011;11:351.
610 17. Faulkes CG, Trowell SN, Jarvis JU, Bennett NC. Investigation of numbers and motility of
611 spermatozoa in reproductively active and socially suppressed males of two eusocial African
612 mole-rats, the naked mole-rat (Heterocephalus glaber) and the Damaraland mole-rat
613 (Cryptomys damarensis). J Reprod Fertil. 1994;100:411–6. doi:10.1530/jrf.0.1000411.
614 18. Abbott DH, Hodges JK, George LM. Social status controls LH secretion and ovulation in
615 female marmoset monkeys (Callithrix jacchus). J Endocrinol. 1988;117:329–39.
616 doi:10.1677/joe.0.1170329.
617 19. White S, Nguyen T, Fernald RD. Social regulation of gonadotropin-releasing hormone. J
618 Exp Biol. 2002;205:2567–81.
619 20. Skulachev VP, Holtze S, Vyssokikh MY, Bakeeva LE, Skulachev M V., Markov A V., et al.
620 Neoteny, Prolongation of Youth: From Naked Mole Rats to "Naked Apes" (Humans). Physiol
621 Rev. 2017;97:699–720. doi:10.1152/physrev.00040.2015.
622 21. Sherman PW, Jarvis JUM, Alexander RD. Reproduction in Naked Mole-Rats. In: The
623 Biology of the Naked Mole-rat. Princeton University Press; 1991. p. 384–425.

624 22. Dengler-Crish CM, Catania KC. Phenotypic plasticity in female naked mole-rats after
625 removal from reproductive suppression. J Exp Biol. 2007;210 Pt 24:4351–8.
626 23. Pinto M, Jepsen KJ, Terranova CJ, Buffenstein R. Lack of sexual dimorphism in femora of
627 the eusocial and hypogonadic naked mole-rat: a novel animal model for the study of delayed
628 puberty on the skeletal system. Bone. 2010;46:112–20. doi:10.1016/j.bone.2009.08.060.
629 24. Peroulakis ME, Goldman B, Forger NG. Perineal muscles and motoneurons are sexually
630 monomorphic in the naked mole-rat (Heterocephalus glaber). J Neurobiol. 2002;51:33–42.
631 25. Sherman PW, Jarvis JUM, Alexander RD. An Ethogram for the Naked Mole-Rat: Nonvocal
632 Behaviors. In: The Biology of the Naked Mole-rat. Princeton University Press; 1991. p. 209–42.
633 26. Sancak Y, Peterson TR, Shaul YD, Lindquist RA, Thoreen CC, Bar-Peled L, et al. The Rag
634 GTPases Bind Raptor and Mediate Amino Acid Signaling to mTORC1. Science (80-).
635 2008;320:1496–501. http://science.sciencemag.org/content/320/5882/1496.abstract.
636 27. Zoncu R, Efeyan A, Sabatini DM. mTOR: from growth signal integration to cancer,
637 diabetes and ageing. Nat Rev Mol Cell Biol. 2011;12:21–35. doi:10.1038/nrm3025.
638 28. Millay DP, O/'Rourke JR, Sutherland LB, Bezprozvannaya S, Shelton JM, Bassel-Duby R,
639 et al. Myomaker is a membrane activator of myoblast fusion and muscle formation. Nature.
640 2013;499:301–5. http://dx.doi.org/10.1038/nature12343.
641 29. Stoll EA, Karapavlovic N, Rosa H, Woodmass M, Rygiel K, White K, et al. Naked mole-
642 rats maintain healthy skeletal muscle and Complex IV mitochondrial enzyme function into
643 old age. Aging (Albany NY). 2016. doi:10.18632/aging.101140.
644 30. Holtze S, Eldarov CM, Vays VB, Vangeli IM, Vysokikh MY, Bakeeva LE, et al. Study of
645 age-dependent structural and functional changes of mitochondria in skeletal muscles and
646 heart of naked mole rats (Heterocephalus glaber). Biochem. 2016;81:1429–37.
647 doi:10.1134/S000629791612004X.
648 31. Craig T, Smelick C, Tacutu R, Wuttke D, Wood SH, Stanley H, et al. The Digital Ageing

649 Atlas: integrating the diversity of age-related changes into a unified resource. Nucleic Acids
650 Res. 2014;43:D873--D878. doi:10.1093/nar/gku843.
651 32. Cellerino A, Ori A. What have we learned on aging from omics studies? Seminars in Cell
652 and Developmental Biology. 2017.
653 33. Bustos V, Partridge L. Good Ol' Fat: Links between Lipid Signaling and Longevity. Trends
654 in Biochemical Sciences. 2017.
655 34. Narendra DP, Jin SM, Tanaka A, Suen D-F, Gautier CA, Shen J, et al. PINK1 Is Selectively
656 Stabilized on Impaired Mitochondria to Activate Parkin. PLOS Biol. 2010;8:e1000298.
657 http://dx.doi.org/10.1371%2Fjournal.pbio.1000298.
658 35. Safdar A, deBeer J, Tarnopolsky MA. Dysfunctional Nrf2-Keap1 redox signaling in
659 skeletal muscle of the sedentary old. Free Radic Biol Med. 2010;49:1487–93.
660 36. Baumgart M, Priebe S, Groth M, Hartmann N, Menzel U, Pandolfini L, et al. Longitudinal
661 RNA-Seq Analysis of Vertebrate Aging Identifies Mitochondrial Complex I as a Small-
662 Molecule-Sensitive Modifier of Lifespan. Cell Syst. 2016;2:122–32.
663 doi:10.1016/j.cels.2016.01.014.
664 37. Miwa S, Jow H, Baty K, Johnson A, Czapiewski R, Saretzki G, et al. Low abundance of the
665 matrix arm of complex I in mitochondria predicts longevity in mice. Nat Commun. 2014;5.
666 38. Hühne R, Thalheim T, Sühnel J. AgeFactDB - The JenAge Ageing Factor Database -
667 Towards data integration in ageing research. Nucleic Acids Res. 2014;42:892–6.
668 39. Dai H, Leeder JS, Cui Y. A modified generalized Fisher method for combining
669 probabilities from dependent tests. Front Genet. 2014;5:32. doi:10.3389/fgene.2014.00032.
670 40. Roellig K, Drews B, Goeritz F, Hildebrandt TB. The long gestation of the small naked
671 mole-rat (Heterocephalus glaber Rüppell, 1842) studied with ultrasound biomicroscopy and
672 3D-ultrasonography. PLoS One. 2011;6:e17744.
673 41. Peaker M, Taylor E. Sex ratio and litter size in the guinea-pig. Reproduction. 1996;108:63–

674 7. doi:10.1530/jrf.0.1080063.

675 42. Yu C, Li Y, Holmes A, Szafranski K, Faulkes CG, Coen CW, et al. RNA sequencing reveals
676 differential expression of mitochondrial and oxidation reduction genes in the long-lived
677 naked mole-rat when compared to mice. PLoS One. 2011;6:e26729.

678 43. Heinze I, Bens M, Calzia E, Holtze S, Dakhovnik O, Sahm A, et al. Species comparison of
679 liver proteomes reveals enhanced lipid metabolism, reduced mitochondrial respiration and
680 enhanced expression of detoxifying enzymes in the long-lived naked mole-rat. bioRxiv. 2017.
681 doi:https://doi.org/10.1101/220343.

682 44. Grossman CJ. Interactions between the gonadal steroids and the immune system. Science.
683 1985.

684 45. Faulkes CG, Abbott DH, Jarvis JU, Sherriff FE. LH responses of female naked mole-rats,
685 Heterocephalus glaber, to single and multiple doses of exogenous GnRH. Reproduction.
686 1990;89:317–23. doi:10.1530/jrf.0.0890317.

687 46. Gesquiere LR, Learn NH, Simao MCM, Onyango PO, Alberts SC, Altmann J. Life at the
688 Top: Rank and Stress in Wild Male Baboons. Science (80-). 2011;333:357–60.
689 doi:10.1126/science.1207120.

690 47. O'Connor CM, Rodela TM, Mileva VR, Balshine S, Gilmour KM. Corticosteroid receptor
691 gene expression is related to sex and social behaviour in a social fish. Comp Biochem Physiol
692 A Mol Integr Physiol. 2013;164:438–46. doi:10.1016/j.cbpa.2012.12.003.

693 48. Crump CJ, Chevins PF. Prenatal stress reduces fertility of male offspring in mice, without
694 affecting their adult testosterone levels. Horm Behav. 1989;23:333–43.
695 http://www.ncbi.nlm.nih.gov/pubmed/2793076. Accessed 21 Mar 2017.

696 49. Clarke FM, Faulkes CG. Dominance and queen succession in captive colonies of the
697 eusocial naked mole-rat, Heterocephalus glaber. Proc R Soc London B Biol Sci. 1997;264:993–
698 1000. doi:10.1098/rspb.1997.0137.

699 50. Clarke FM, Faulkes CG. Hormonal and behavioural correlates of male dominance and
700 reproductive status in captive colonies of the naked mole-rat, Heterocephalus glaber. Proc
701 Biol Sci. 1998;265:1391–9. doi:10.1098/rspb.1998.0447.
702 51. Maruska KP, Fernald RD. Plasticity of the reproductive axis caused by social status change
703 in an african cichlid fish: II. Testicular gene expression and spermatogenesis. Endocrinology.
704 2011;152:291–302.
705 52. Bens M, Sahm A, Groth M, Jahn N, Morhart M, Holtze S, et al. FRAMA: from RNA-seq
706 data to annotated mRNA assemblies. BMC Genomics. 2016;17:54. doi:10.1186/s12864-015-
707 2349-8.
708 53. Grabherr MG, Haas BJ, Yassour M, Levin JZ, Thompson DA, Amit I, et al. Full-length
709 transcriptome assembly from RNA-Seq data without a reference genome. Nat Biotechnol.
710 2011;29:644–52.
711 54. Keane M, Craig T, Alfoldi J, Berlin a. M, Johnson J, Seluanov A, et al. The Naked Mole Rat
712 Genome Resource: facilitating analyses of cancer and longevity-related adaptations.
713 Bioinformatics. 2014;30:3558–60. doi:10.1093/bioinformatics/btu579.
714 55. Kent WJ. BLAT - The BLAST-like alignment tool. Genome Res. 2002;12:656–64.
715 56. Kapustin Y, Souvorov A, Tatusova T, Lipman D. Splign: algorithms for computing spliced
716 alignments with identification of paralogs. Biol Direct. 2008;3:20.
717 57. Dobin A, Davis C a., Schlesinger F, Drenkow J, Zaleski C, Jha S, et al. STAR: Ultrafast
718 universal RNA-seq aligner. Bioinformatics. 2013;29:15–21.
719 58. Anders S, Pyl PT, Huber W. HTSeq-A Python framework to work with high-throughput
720 sequencing data. Bioinformatics. 2015;31:166–9.
721 59. Langmead B, Salzberg SL. Fast gapped-read alignment with Bowtie 2. Nat Methods.
722 2012;9:357–9. doi:10.1038/nmeth.1923.
723 60. Love MI, Huber W, Anders S. Moderated estimation of fold change and dispersion for

724 RNA-seq data with DESeq2. Genome Biol. 2014;15:550. doi:10.1186/s13059-014-0550-8.

725 61. Kasen S, Ouellette R, Cohen P. Mainstreaming and postsecondary educational and
726 employment status of a rubella cohort. Am Ann Deaf. 1990;135:22–6. doi:10.2307/2346101.

727 62. Zeeberg BR, Feng W, Wang G, Wang MD, Fojo AT, Sunshine M, et al. GoMiner: a resource
728 for biological interpretation of genomic and proteomic data. Genome Biol. 2003;4:R28.
729 doi:10.1186/gb-2003-4-4-r28.

730 63. Supek F, Bošnjak M, Škunca N, Šmuc T. REVIGO summarizes and visualizes long lists of
731 gene ontology terms. PLoS One. 2011;6:e21800. doi:10.1371/journal.pone.0021800.

732

733 ## Supplementary Table Legends

734 **Table S1.** Age at death for NMRs and GPs.

735 **Table S2.** Number of analyzed biological replicates per group.

736 **Table S3.** Reason for exclusion of samples from further analysis.

737 **Table S4.** Number of uniquely aligned RNA-seq reads.

738 **Table S5.** Mean pairwise Pearson correlation coefficients between biological replicates in (A)
739 naked mole-rat and (B) guinea pig.

740 **Table S6.** Number of differentially expressed genes (FDR < 0.01) between NMR and GP
741 (A) without logFC threshold and (B) with logFC threshold (|logFC| > 2).

742 **Table S7.** DEGs in cross-species comparison that show an overlap with DAA.

743 **Table S8.** Gene set enrichment analysis for cross-species DEGs (FDR < 0.01, |logFC| > 2) that
744 are age-related (DAA).

745 **Table S9.** Number of sex-related (female vs. male) differentially expressed genes in (A) non-
746 breeder and (B) breeder (FDR < 0.01).

747 **Table S10.** Functional enrichment analysis of 790 DEGs shared between GP-B-FvM and GP-
748 N-FvM.

749 **Table S11.** Gene description of sex-related DEGs in NMR-N-FvM.

750 **Table S12.** Number of status-related (breeder vs. non-breeder) differentially expressed genes
751 in (A) females and (B) males (FDR < 0.01).

752 **Table S13.** Functional gene set enrichment analysis of DEGs in Ovr of NMR-F-BvsN.

753 **Table S14.** Functional gene set enrichment analysis of DEGs in Adr of NMR-F-BvsN.

754 **Table S15.** Functional gene set enrichment analysis of DEGs in Cer of NMR-F-BvsN.

755 **Table S16.** DEGs in intersection between NMR-F-BvsN and NMR-M-BvsN.

756 **Table S17.** Functional gene set enrichment analysis of DEGs in Tes of NMR-M-BvsN.

757 **Table S18.** Functional enrichment analysis in cellular components of DEGs in Tes
758 NMR-M-BvsN.

759 **Table S19.** Functional gene set enrichment analysis of DEGs in Skn of NMR-M-BvsN.

760 **Table S20.** Proportion of mitochondrial transcriptonal output.

761 **Table S21.** Differentially expressed nuclear genes (FDR<0.05) associated with mitochondrial
762 respiratory chain complexes in Tes and Skn of NMR-M-BvsN.

763 **Table S22.** Antioxidant enzymes differentially expressed in Tes and Skn of
764 NMR-M-BvsN (FDR<0.05).

765 **Table S23.** Enrichment of age-related genes (Digital Ageing Atlas) in status-related DEGs.
766 Only tissues having at least 50 DEGs were tested for enrichment.

767 **Table S24.** Shared status-related genes between NMR and GP.

768 **Table S25.** FDR values (Fisher's exact test) for overlap between Digital Ageing Atlas and
769 upper quintile of status-related expression differences having the greatest interspecies
770 difference. Three groups were investigated: (i) opposing and (ii) same direction of expression
771 in both species as well as (iii) independent of direction. Further, in each group direction in
772 each species was tested separately.

773 **Table S26.** Functional enrichment analysis of the non-redundant set of aging-related
774 20%-quantiles that show the greatest interspecies difference in males (Skn, Tes).

775 **Table S27.** Functional enrichment analysis of the non-redundant set of aging-related
776 20%-quantiles that show the greatest interspecies difference in females (Hrt, Pit, Ovr).
777

778 Supplementary Figure Legends

779 **Figure S1:** Collected tissues exemplified in schematic figure of NMR.

780 **Figure S2:** Hierarchical clustering of gene expression profiles. The clustering tree shows a
781 clear separation of tissues in both species, but less pronounced differences between sex and
782 breeding status.

783 **Figure S3:** Top 15 highest ranked GO sets based on enrichment analysis of cross-species
784 DEGs between NMR and GP. GO sets are ranked by number of summarized GO terms (x-
785 axes) and number of DEGs (alongside bar).

786 **Figure S4:** Top 15 highest ranked GO sets based on enrichment analysis of sex-related DEGs
787 that are shared between GP breeder and non-breeder. GO sets are ranked by number of
788 summarized GO terms (x-axes) and number of DEGs (alongside bar).

789 **Figure S5:** Top 15 highest ranked GO sets based on enrichment analysis of sex-related DEGs
790 in NMR breeder. GO sets are ranked by number of summarized GO terms (x-axes) and
791 number of DEGs (alongside bar, together with number of up- and downregulated genes).

792 **Figure S6:** Top 15 highest ranked GO sets based on enrichment analysis of status-related
793 DEGs in ovary of NMR females. GO sets are ranked by number of summarized GO terms
794 (x-axes) and number of DEGs (alongside bar, together with number of up- and
795 downregulated genes).

796 **Figure S7:** Top 15 highest ranked GO sets based on enrichment analysis of status-related
797 DEGs in adrenal gland of NMR females. GO sets are ranked by number of summarized GO

terms (x-axes) and number of DEGs (alongside bar, together with number of up- and downregulated genes).

Figure S8: Top 15 highest ranked GO sets based on enrichment analysis of status-related DEGs in cerebellum of NMR females. GO sets are ranked by number of summarized GO terms (x-axes) and number of DEGs (alongside bar, together with number of up- and downregulated genes).

Figure S9: Top 15 highest ranked GO sets based on enrichment analysis of status-related DEGs in testis of NMR males. GO sets are ranked by number of summarized GO terms (x-axes) and number of DEGs (alongside bar, together with number of up- and downregulated genes).

Figure S10: Top 15 highest ranked GO sets based on enrichment analysis of status-related DEGs in skin of NMR males. GO sets are ranked by number of summarized GO terms (x-axes) and number of DEGs (alongside bar, together with number of up- and downregulated genes).

Figure S11: Mitonuclear ratios in non-breeders and breeders per sex, tissue and species. Boxplots shows median, 2nd/3rd quartiles, whiskers extend to 1.5 the interquartile range and dots values outside this range. P-values were calculated using a two-tailed t-test; *: $p<0.05$, **: $p<0.01$.

Figure S12: Top 15 highest ranked GO sets based on enrichment analysis of the non-redundant set of aging-related 20%-quantiles that show the greatest interspecies difference in males (Tes, Skn). GO sets are ranked by number of summarized GO terms (x-axes) and number of DEGs (alongside bar).

820 **Figure S13:** Top 15 highest ranked GO sets based on enrichment analysis of the non-
821 redundant set of aging-related 20%-quantiles that show the greatest interspecies difference in
822 females (Hrt, Pit, Ovr). GO sets are ranked by number of summarized GO terms (x-axes) and
823 number of DEGs (alongside bar).

824 **Supplemental Text S1**

825 In NMR-M-BvsN Tes, this is indicated by a significant upregulation of receptors for
826 androgens (AR, 1.3-fold) and gonadotrophic hormones (LHCGR, 1.8-fold) as well as an
827 increase in steroid production. Specifically, we observe an upregulation of genes involved in
828 the transport of cholesterol into mitochondria (STAR, steroidogenic acute regulatory protein,
829 2.8-fold; TSPO, translocator protein, 1.5-fold; CAV1, caveolin 1, 1.4-fold), the rate limiting step
830 of steroidogenesis (1), and conversion of cholesterol into pregnenolone (CYP11A1,
831 cytochrome P450 family 11 subfamily A member 1, 1.8-fold), which is essential for all
832 steroids. Genes encoding for enzymes that produce testosterone (HSD17B1, hydroxysteroid
833 17-beta dehydrogenase 1, 1.4-fold), the more potent metabolite dihydrotestosterone (SRD5A1,
834 steroid 5 alpha-reductase 1, 1.3-fold) and cortisol (CYP51A1, cytochrome P450 family 51
835 subfamily A member 1, 2-fold) are upregulated as well (Supplement Figure 10). The
836 upregulation of steroidogenesis is accompanied by a significant increase in the mitonuclear
837 ratio and enrichment of nuclear DEGs associated with mitochondria, including OXPHOS.
838 Consequently, the load of reactive oxygen species (ROS) is presumably higher in NMR Tes,
839 but is compensated by increase in antioxidant enzymes. NMR-F-BvsN Ova shows more
840 subtle changes in steroidogenesis by increased estradiol production as indicated by
841 significant upregulation of CYP19A1 (aromatase, 2.5-fold) and increased sensitivity to
842 androgens and progesterogens as indicated by upregulation of corresponding receptors (Ova,
843 AR, 1,4-fold; Pit, PGR, 1.6-fold). We find, however, substantial expression changes in two

844 genes involved in the regulation of follicle-stimulating hormone secretion (2), INHA (inhibin
845 alpha subunit, 19.2-fold) and INHBA (inhibin beta A subunit, 4.4-fold), indicating that ovaries
846 of non-breeding NMRs lack preovulatory follicles. Further, enrichment of steroid metabolic
847 process, response to hormones and prostate gland growth indicates active feedback signalling
848 also in females and an impact on developmental processes. Increase in signalling is further
849 supported by significant enrichment of gene products located in secretory vesicle (secretory
850 granule lumen, GO:0034774) and on cell surface (GO:0009986).

851 **References**

852 1. Stocco DM, Clark BJ (1996) Regulation of the acute production of steroids in
853 steroidogenic cells. Endocr Rev 17(3):221–244.

854 2. Wijayarathna R, de Kretser DM (2016) Activins in reproductive biology and beyond.
855 Hum Reprod Update 22(3):dmv058.

856 Supplemental Text S2

857 Although well expressed, we found no significant differences for gonadotropin-related genes
858 (GNRH1, FSHB, CGA, LHB). This indicates a similar intracellular transcript turnover in non-
859 breeders and breeders, and is consistent with previous results indicating that LH is stored in
860 non-breeders, ready to be released upon GnRH signalling (1). Notably, GnIH (NPVF), a
861 negative regulator of reproductive function suggested to have a role in reproductive
862 immaturity in NMRs due to its decreased protein expression in brain of NMR breeder (2),
863 shows tendentially decreased mRNA expression in NMR breeders (males: 0.37, females
864 0.13). Also, previously elevated diencephalon mRNA levels in NMR were reported for AR
865 (androgen receptor) in male breeders and for CYP19A1 (aromatase), ESR1 (estrogen receptor
866 1) and PGR (progesterone receptor) in female breeders (3). Our corresponding Hyp data do

867 not support those increases (log2FC<0.1). Nevertheless, we identified significantly elevated
868 transcript levels of these genes both in male (Tes: AR; Supplemental Data S67) and female
869 breeders (Pit: PGR, Supplemental Data S54; Ova: AR, CYP19A1, ESR1, PGR, Supplemental
870 Data S57) supporting a complex status-related function of these genes. Furthermore, steroid
871 feedback and GnRH secretion are integrated by brain GABA and glutamate signalling in
872 mammals and cichlids (4). Although, we do not observe equivalent significant differences in
873 the NMR brain, the data show an upregulation of genes coding for three GABA receptor
874 subunits (GABRB3, GABRG1, GABRP) and one glutamate receptor subunit (GRIK2) in Tes
875 (Supplemental Data S67), as well as two of three differentially expressed GABA (GABRB2,
876 GABRG3) and three glutamate receptor subunits (GRIK1, GRIK2, GRIK4) in Ova and female
877 Pit of NMR breeders (Supplemental Data S54, S57). Together, this suggests increased
878 neuronal plasticity and/or activity predominantly in gonads of NMRs after becoming
879 breeders.

880 In the testis of immature chicken, expression of ADIPOR1/2 (adiponectin receptor 1/2) is
881 significantly lower than in mature animals (5). It has been hypothesised that these genes are
882 involved in supporting the higher metabolic activity related to spermatogenesis, testicular
883 steroid hormone production, and transport of spermatozoa and testicular fluid. In line with
884 these observations, our results show a significant upregulation of ADIPOR2 in Tes of NMR
885 breeders (1.7-fold; Supplemental Data S67).

886 The renin-angiotensin system predominantly involved in cardiovascular control has also been
887 associated with reproduction in mice and human (6). Signaling through receptors coded by
888 AGTR1 (angiotensin II receptor type 1) in males, and AGTR1/2 in females has been associated
889 with fertility and stimulation of reproduction. In accordance, we observed a significant

890 upregulation of AGTR1 and AGTR2 in gonads of NMR male and female breeders,
891 respectively (Supplemental Data S67,S57).

892 **References**

893 1. Faulkes CG, Abbott DH, Jarvis JU, Sherriff FE (1990) LH responses of female naked
894 mole-rats, Heterocephalus glaber, to single and multiple doses of exogenous GnRH.
895 Reproduction 89(1):317–323.

896 2. Peragine DE, et al. (2017) RFamide-related peptide-3 (RFRP-3) suppresses sexual
897 maturation in a eusocial mammal. Proc Natl Acad Sci 3:201616913.

898 3. Swift-Gallant A, Mo K, Peragine DE, Monks DA, Holmes MM (2015) Removal of
899 reproductive suppression reveals latent sex differences in brain steroid hormone receptors in
900 naked mole-rats, Heterocephalus glaber. Biol Sex Differ 6(1):31.

901 4. Renn SCP, Aubin-Horth N, Hofmann H a (2008) Fish and chips: functional genomics
902 of social plasticity in an African cichlid fish. J Exp Biol 211(Pt 18):3041–3056.

903 5. Ocón-Grove OM, Krzysik-Walker SM, Maddineni SR, Hendricks GL, Ramachandran
904 R (2008) Adiponectin and its receptors are expressed in the chicken testis: influence of sexual
905 maturation on testicular ADIPOR1 and ADIPOR2 mRNA abundance. Reproduction
906 136(5):627–38.

907 6. Pan PP, Zhan QT, Le F, Zheng YM, Jin F (2013) Angiotensin-converting enzymes play
908 a dominant role in fertility. Int J Mol Sci 14(10):21071–21086.

909